

GEOMETRIC CONSISTENCY AND STABILITY OF CONSUMER-GRADE DIGITAL CAMERAS FOR ACCURATE SPATIAL MEASUREMENT

RENE WACKROW (r.wackrow@lboro.ac.uk)

JIM H. CHANDLER (j.h.chandler@lboro.ac.uk)

Loughborough University

PAUL BRYAN (paul.bryan@english-heritage.org.uk)

English Heritage

Abstract

It is known that uncertain internal geometry of consumer-grade digital cameras limits the accuracy of data that can be extracted. These cameras can be calibrated, but the validity of calibration data over a period of time should be carefully assessed before subsequent photogrammetric measurement. This paper examines the geometric stability and manufacturing consistency of a typical low-cost digital camera (Nikon Coolpix 5400) by estimating the degree of similarity between interior orientation parameters (IOP), established over a 1-year period. Digital elevation models (DEMs) were extracted with differing IOP, and accuracies were compared using data obtained from seven identical cameras. An independent self-calibrating bundle adjustment (GAP) and the Leica Photogrammetry Suite (LPS) software were used to provide these data-sets. Results are presented that indicate the potential of these cameras to maintain their internal geometry in terms of temporal stability and manufacturing consistency. This study also identifies residual systematic error surfaces or “domes”, discernible in “DEMs of difference”. These are caused by slightly inaccurately estimated lens distortion parameters, which effectively constrain the accuracies achievable with this class of sensor.

KEYWORDS: camera calibration, camera stability, close range photogrammetry, digital cameras

INTRODUCTION

THE MAIN ADVANTAGES of consumer-grade digital cameras are their convenience, portability and low cost. These cameras have not been traditionally used for photogrammetric measurements, owing to their uncertain geometry. The uncertainties can be partially resolved by calibration but their temporal stability and manufacturing consistency remain unknown.

During a collaborative project with English Heritage to record rock art in the north-east of England (Chandler et al., 2007), seven identical Nikon Coolpix 5400 digital cameras (Fig. 1) were calibrated. This provided the opportunity to assess their stability over a 1-year period as well as their consistency of manufacture.



FIG. 1. Nikon Coolpix 5400.

Previous work related to calibration of consumer-grade cameras is reviewed, before describing the methodology adopted for the study. The link between the stability analyses strategy and the reconstructed object space is introduced followed by experimental results and discussion. Finally, this paper concludes with a brief summary and recommendations for future work.

PREVIOUS WORK ON CALIBRATION OF CONSUMER-GRADE CAMERAS

Over the past decade, several researchers have assessed the photogrammetric potential of non-metric digital cameras. The Kodak DCS420 and DCS460 have been tested in a variety of photogrammetric applications (Beyer et al., 1995; Brown and Dold, 1995; Fraser et al., 1995; Peipe, 1995; Dold and Peipe, 1996; Miyatsuka, 1996; Schneider, 1996; Shortis et al., 1998; Ahmad and Chandler, 1999) and the use of similar cameras such as the Kodak DC40 has been described in Miyatsuka (1996) and Lichti and Chapman (1997). In addition, the suitability for close range measurement of the Kodak DCS Pro Back used in conjunction with the Mamiya body was reported in Mills et al. (2003). The accuracies in close range surface measurement of three low-cost consumer-grade digital cameras (Sony DSC-P10, Olympus C3030, Nikon Coolpix 3100) and the Kodak DCS460 have been compared in Chandler et al. (2005). All cameras tested revealed potential for use in close range photogrammetry where low to medium accuracy was required. The use of consumer-grade digital cameras for photogrammetric measurements is increasingly accepted in many industrial applications but also in diverse fields ranging from medical and forensic science to architectural work (Fryer et al., 2007).

The stability of non-metric digital cameras has been reported less frequently in the literature. Shortis et al. (2001) introduced a strategy for accessing the stability of a digital camera by using the ratio of the mean precision of target coordinates to the largest dimension of the target array. Habib and Morgan (2005) attributed the lack of literature to the absence of standards for quantitative analyses of camera stability. An approach based on statistical testing of two sets of interior orientation parameters (IOP) was presented and the disadvantages of this strategy were discussed. Due to the drawbacks of this methodology, a new procedure for stability analysis based on the degree of similarity between the reconstructed bundles using two sets of IOP was introduced. The stability of the Olympus C-5050 digital camera was reported in Bosch et al. (2005). This was achieved by comparing the coordinates of check points with coordinates acquired with a total station. This test was not independent because the same points were used to determine the exterior orientation. Three methodologies (ZROT, ROT and SPR) for evaluating the stability of a camera are presented in Habib et al. (2006). The procedures impose constraints regarding the exterior orientation of the bundles compared. Therefore, each is applicable for a specific georeferencing technique which describes the position and orientation of the images relative to a coordinate system.

This review of previous work identified the need for an appropriate method to assess the temporal stability and manufacturing consistency of consumer-grade digital cameras. A suitable approach which achieves this objective is described in this paper.

STABILITY ANALYSES OF SEVEN NIKON COOLPIX 5400 CAMERAS

Consumer-grade digital cameras have not been designed for measurement, so their internal geometry is generally considered unstable (Shortis et al., 1998). The aim of stability analyses is to determine whether the interior orientation of a camera changes over time or not. The methodology adopted initially in this study was to evaluate the degree of similarity between two sets of IOP. In addition, the impact of varying IOP on accuracy in the object space was assessed; this is ultimately of more significance to most users.

The Cameras

Seven Nikon Coolpix 5400 digital cameras were purchased by the Northumberland and Durham Rock Art Project in February 2005 (Barnett, 2006). These have been used regularly by teams of volunteers to systematically record 1500 rock art motifs located in the north of England (Chandler et al., 2007). The need to calibrate these seven cameras provided the opportunity to evaluate the stability and consistency of these sensors during normal operation in field conditions. It was judged that there was no further need to simulate disturbing impacts of the camera geometry, such as variations in temperature and moisture, external forces on the camera body or use of the auto-focus device. A benefit of the presence of seven identical cameras was that manufacturing consistency could also be assessed. A detailed overview of the characteristics of the Nikon Coolpix 5400 camera is given in Table I.

The Testfield

It was expected that the seven cameras would mainly be used at an object distance of 1.5 m for rock art recording. Therefore, a 3D and planar testfield was specifically constructed to allow the cameras to be calibrated at this distance. It is an enhancement of the testfield used in Chandler et al. (2005) and consists of a medium density fibreboard (MDF) (1.2 m × 0.9 m) to which eight square blocks of various shapes and heights were added (Fig. 2). These blocks replicate physical structures such as buildings found in normal vertical aerial photography. To provide an appropriate texture for the image-matching algorithm included in the Leica Photogrammetry Suite (LPS) software, the MDF board was painted white and finally splattered

TABLE I. Characteristics of the Nikon Coolpix 5400 camera.

<i>Feature</i>	<i>Nikon Coolpix 5400</i>
Camera body	Compact
Resolution [pixel]	5 million
Image size [pixel]	2592 × 1944
Size of sensor [mm]	7.18 × 5.32
Size of pixel [μm]	2.77 × 2.77
Auto focus	Yes
Manual focus	Yes
Dimensions [mm]	108 × 73 × 69
Weight [kg]	0.4
Cost [£]	240 (January 2005)

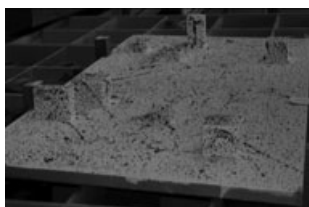


FIG. 2. Test object.

with red and blue paint. This test object provides the opportunity to derive thousands of object measurements; by comparing elevations with their known values, a similar number of check points can be achieved. This allows the accuracy in the object space to be determined with good statistical reliability. In addition, 28 photogrammetric target points were distributed over the testfield (Fig. 3) and coordinated by theodolite intersection using a Leica TC1010 total station (June 2005). The measurements, both horizontal and vertical angles and the distance between the two theodolite stations, were initially computed using basic intersection formulae. The estimates of the coordinates of the target points, the measurements derived using a total station and a subset of distances measured with a steel band were then combined in a least squares “variation of coordinates” adjustment to determine the best estimates for the photogrammetric target points. These coordinates were used to create a digital elevation model (DEM) at 1 mm resolution, known as the “Truth DEM”. Another set of coordinates was derived by repeating the procedure in May 2006. Both sets of coordinates were compared using a 3D similarity transformation. The residuals (maximum 0.5 mm) demonstrate the geometric stability of the testfield over time; thus any deviations between similarly derived IOP cannot be attributed to distortion of the MDF base material.

Camera Calibration

Determination of the geometric conditions of a camera, described by the IOP, is known as camera calibration. Methods of camera calibration have evolved over the past few decades, through the development of computational techniques and because of the increasing use of non-metric digital cameras for photogrammetric measurements. The widely used method of self-calibration, where all image observations from various camera positions are used to determine the unknown interior and exterior orientation parameters (Clarke and Fryer, 1998), was adopted in this research.

Six frames, representing the whole test object, were captured with each of the seven cameras at a camera-to-object distance of approximately 1.5 m (Fig. 4), with the camera focus set on infinity. The same basic configuration was used for each camera at each time.

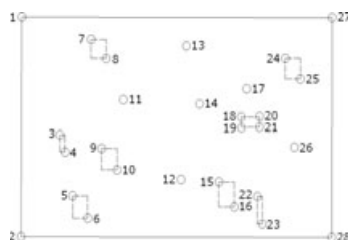


FIG. 3. Position of photogrammetric target points.

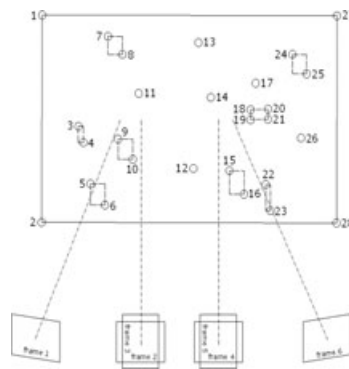


FIG. 4. Image geometry.

For processing the images in the LPS, it was essential initially to define the primary orientation of the sensor. The readily accessible <http://www.dpreview.com> website was used to identify the physical size of the sensor and consequently the physical size of each pixel of the CCD array in the x and y directions. Once the pixel size and an approximate focal length were defined, the point measurement tool of LPS was used to measure 11 photogrammetric target points manually before 100 tie points were measured using fully automated methods.

Previous work conducted by Chandler et al. (2005) demonstrated that the external self-calibrating bundle adjustment GAP (Chandler and Clark, 1992) can also be used to estimate the camera parameters; this was also used in these studies to provide another approach independent of LPS. A familiar eight-parameter model for the bundle adjustment (Kenefick et al., 1972) was available which includes parameters for principal distance, principal point offset and corrections for radial and decentring distortion. The program can also estimate two additional parameters for affinity and differential scale, but were not found necessary in this study. Avoiding solutions which are overparameterised is important (Granshaw, 1980; Fraser, 1982) and the significance of additional parameters was assessed by comparing them with their stochastic properties. This demonstrated that two parameters (k_1 , k_2) were significant for modelling radial distortion. However, k_3 and the parameters (p_1 , p_2) used for modelling the decentring distortion proved insignificant and were removed. This five-parameter model for the self-calibrating bundle adjustment was maintained for all seven cameras. The derived inner orientation parameters were then re-established into LPS for the purpose of deriving high-resolution DEMs and check point data.

DEM Generation

The LPS software was used for DEM generation by means of a hierarchical feature-based matching algorithm (ERDAS, 2002). Tests revealed that DEMs with optimum accuracy were produced using the following strategy:

DTM cell size:	0.003 m \times 0.003 m
Search size:	7 \times 3
Correlation size:	7 \times 7
Coefficient limit:	0.80
Topographic type:	Flat terrain
Object type:	Open area
DTM filtering:	High

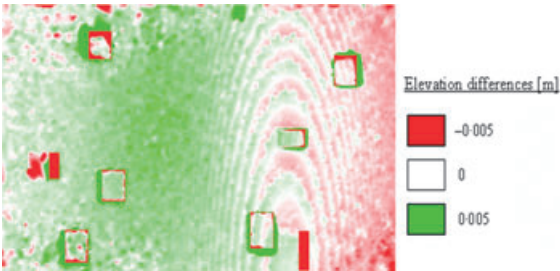


FIG. 5. Elevation differences—IOP: 4th July 2005.

The adaptive capability of LPS to change the search size, correlation size and correlation coefficient limit dynamically during DEM generation was switched off for simplicity.

The automatically extracted DEMs, representing the whole of the physical test object, were compared with the “Truth DEM” by interpolation and subtraction to produce DEMs of difference. As recommended by Li (1988), mean error and standard deviation of error of DEMs of difference were derived using an ERDAS Graphical Model. Tests demonstrated that significant areas of inaccurate DEM are situated adjacent to the wooden blocks, which clearly illustrated the shadowing effect of them (Fig. 5). These effects obviously distorted the accuracy statistics. In order to avoid this distortion, statistics were also computed for an area of interest which represented the central and flat part of the test object and did not include the wooden blocks. The optimum accuracy for each DEM of difference could consequently be quantified.

RESULTS

Temporal Stability

The temporal stability of the Nikon Coolpix 5400 camera can be assessed by comparing the degree of similarity between sets of IOP established at various dates. Seven identical cameras were calibrated on 4th July 2005. This was repeated after 4 days and after a period of approximately 1 year. Table II summarises the accuracy of the calibration procedure in terms of accuracy of fit to the control points (restitution accuracy) of camera 5. Similar results were

TABLE II. Restitution accuracy by using IOP from different dates.

Camera/Imagery date	IOP date	Object rms error [mm]			Image rms error [pixel]	
		X	Y	Z	x	y
Camera 5						
4th July 2005	4th July 2005	0.3	0.2	0.4	0.63	0.55
4th July 2005	8th July 2005	0.2	0.2	0.2	0.63	0.57
4th July 2005	12th July 2006	0.5	0.4	0.4	0.68	0.69
8th July 2005	8th July 2005	0.4	0.2	0.3	0.80	0.82
8th July 2005	4th July 2005	0.2	0.2	0.3	0.79	0.85
8th July 2005	12th July 2006	0.4	0.3	0.4	0.90	0.87
12th July 2006	12th July 2006	0.4	0.3	0.4	0.96	0.82
12th July 2006	4th July 2005	0.3	0.2	0.4	0.94	0.83
12th July 2006	8th July 2005	0.3	0.2	0.4	0.97	0.85

TABLE III. DEM accuracy by using IOP from different dates.

<i>Camera/ Imagery date</i>	<i>IOP date</i>	<i>Full area (mean error \pm standard deviation) [mm]</i>	<i>Central area (mean error \pm standard deviation) [mm]</i>
Camera 5			
4th July 2005	4th July 2005	0.5 \pm 7.2	1.8 \pm 0.9
4th July 2005	8th July 2005	0.4 \pm 5.8	1.1 \pm 0.7
4th July 2005	12th July 2006	0.9 \pm 7.1	2.5 \pm 0.7
8th July 2005	8th July 2005	0.9 \pm 6.1	1.4 \pm 0.8
8th July 2005	4th July 2005	0.6 \pm 6.9	1.3 \pm 1.0
8th July 2005	12th July 2006	1.2 \pm 5.8	1.9 \pm 0.8
12th July 2006	12th July 2006	0.3 \pm 6.0	1.6 \pm 0.7
12th July 2006	4th July 2005	-0.1 \pm 6.6	0.5 \pm 0.9
12th July 2006	8th July 2005	-0.2 \pm 5.6	0.7 \pm 0.7

achieved with the other six cameras; camera 5 will be used as an exemplar. The first column represents the dates of capturing the images of the test object, whilst the second column tabulates the dates of IOP used for restitution. The rms error (mm) in the object space is summarised in columns three to five and the final two columns represent the rms residuals (pixels) in the image space.

The camera achieved sub-millimetre accuracy (average rms error of 0.3 mm), in terms of fit to the control points, whichever combination of image sets and IOP was used. The accuracy statistics indicate no significant variations.

In the image space, accuracies within each set of calibration images varied within the range of approximately 0.1 pixel. However, variations in accuracy at a maximum of 0.4 pixel are noticeable by comparing statistics of different sets of images. This appears to be significant but it must be acknowledged that the automatic tie-point generation tool of LPS was used; this independently creates tie points in each image set. It is plausible that the discrepancies in accuracy are caused by using different sets of tie points in each set of imagery and not by the IOP. This would suggest that there is a high degree of consistency between all sets of IOP for this camera exemplar. A similar result was obtained with the other six cameras.

Table III summarises the accuracy of DEM generation by using different combinations of sets of imagery and IOP at various dates for camera 5 within the two areas of the test object. Similar results were again obtained with the other six cameras. As expected, the cameras achieved poor accuracies for the full test area. These were caused by the small number of gross failures for points adjacent to the wooden blocks. Mean errors for the central area of interest varied from 0.5 to 2.5 mm and did not follow expectations. Even more surprisingly, optimum restitution accuracy was not achieved by generating DEMs using frames and IOP from the same date. This leads to the conclusion that the central area of extracted DEMs was perhaps affected by the same systematic error source, an issue discussed later in this paper.

Consistency of Manufacture

The presence of seven identical Nikon Coolpix 5400 digital cameras provided the opportunity to assess their consistency of manufacture. Three sets of IOP, originally derived with camera 4 in calibration sessions on various dates, were used in conjunction with the six

TABLE IV. Restitution accuracy by using IOP of different cameras/dates.

Camera/Imagery date	Camera/IOP date	Object rms error [mm]			Image rms error [pixel]	
		X	Y	Z	x	y
Camera 5	Camera 5					
4th July 2005	4th July 2005	0.3	0.2	0.4	0.63	0.55
Camera 5	Camera 4					
4th July 2005	4th July 2005	0.4	0.2	0.2	0.68	0.75
4th July 2005	8th July 2005	0.4	0.2	0.4	0.78	0.77
4th July 2005	7th June 2006	0.4	0.3	0.4	0.62	0.57

TABLE V. DEM accuracy by using IOP of different cameras/dates.

Camera/Imagery date	Camera IOP date	Full area	Central area
		(mean error \pm standard deviation) [mm]	(mean error \pm standard deviation) [mm]
Camera 5	Camera 5		
4th July 2005	4th July 2005	0.5 \pm 7.2	1.8 \pm 0.9
Camera 5	Camera 4		
4th July 2005	4th July 2005	0.5 \pm 6.6	1.6 \pm 0.6
4th July 2005	8th July 2005	-0.3 \pm 6.8	0.6 \pm 0.6
4th July 2005	7th June 2006	0.7 \pm 7.1	2.1 \pm 0.9

calibration frames captured with camera 5 on 4th July 2005. The restitution accuracies achieved for these two cameras, which provide a representative sample for the results obtained from all cameras, are presented in Table IV. In particular, no significant discrepancies were observable in the accuracy statistics (average object rms error of 0.3 mm; variation of image rms error of 0.22 pixel) comparing these configurations. It is notable that there is a high degree of similarity between the sets of IOP which certainly demonstrates remarkable geometric consistency achieved by the manufacturer.

The accuracies in the object space, achieved by extracting DEMs using the configurations presented above, are summarised in Table V. This again indicates a poor DEM accuracy estimated for the whole test object and discrepancies between 0.6 and 2.1 mm for the central test area. By comparing the DEM accuracy statistics presented in Tables III and V, it is notable that camera 5 achieved a similar accuracy level, even though IOP sets derived from a different camera were used. This again demonstrates a high degree of manufacturing consistency for this type of camera.

DISCUSSION

DEM Generation and Accuracy Statistics

Figs. 5 to 7 represent DEMs of difference for the full test object using the imagery from 4th July 2005 and IOP sets derived using the 4th and 8th July 2005 and 12th July 2006 imagery, acquired with camera 5. Sets of IOP were achieved using the GAP calibration approach (Chandler et al., 2005). Areas in DEMs with elevations less than -5 mm are illustrated by solid red, while solid green regions indicate height differences greater than +5 mm and white areas represent regions of no height differences between the "Truth DEM" and automatically extracted DEMs.

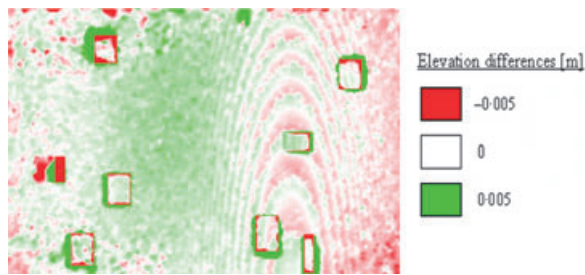


FIG. 6. Elevation differences—IOP: 8th July 2005.

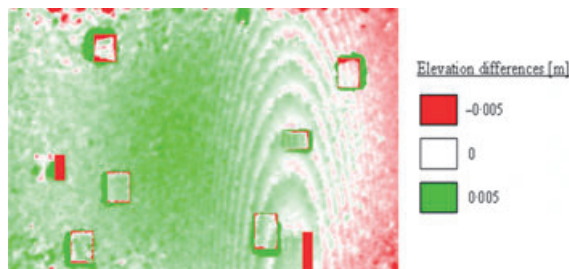


FIG. 7. Elevation differences—IOP: 12th July 2006.

Difference images clearly indicate significant areas of inaccurate DEM which can be classified into four types. Obviously, the DEM generation algorithm of the LPS software has difficulties in extracting information representing the wooden blocks situated on the left and lower right areas of the test object. The dimensions are 70 mm × 30 mm × 100 mm (left block) and 105 mm × 30 mm × 72 mm (lower right block) simulating isolated tall buildings, which perhaps explains these difficulties. Furthermore, areas with gross errors close to the wooden blocks clearly indicate the shadowing effect they cause, which is to be expected. The effect on the numerical statistics can be noticed by comparing the standard deviation (average value 6.3 mm) determined for the full test area with the standard deviation (average value 0.8 mm) for the central region which does not include the wooden blocks. The other obvious areas of inaccurate DEM are the distinctive radial “domes”, slightly shifted to the left and the systematic “contour” pattern to the right of the centre of the DEM. These systematic effects will be accounted for in the next section.

Systematic Pattern in Difference Images

A hierarchical feature-based matching algorithm that incorporates both pyramid layers and an epipolar constraint to reduce the search time for conjugate points in image pairs is used by LPS for DEM generation (ERDAS, 2002). This approach generates a systematic “contour” pattern using a base-to-distance ratio of 1:7 for an image pair, illustrated in Figs. 5 to 7. However, tests have shown that changing the base-to-distance ratio to 1:2 reduces this systematic effect, as demonstrated in Fig. 8. The software manufacturer Leica Geosystems was contacted in November 2006 and this unusual effect was reported. However, no explanation accounting for this pattern has been received to date (May 2007). Tests conducted with another

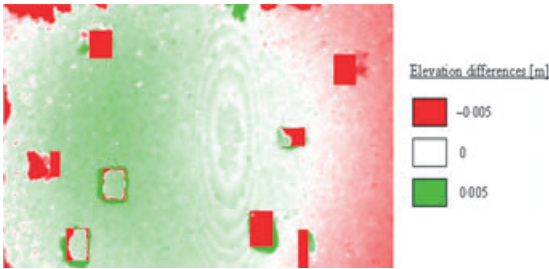


FIG. 8. Difference image with base-to-distance ratio of 1:2.

DEM generation package (ERDAS OrthoMax) created a dome but no such systematic contour pattern.

“Dome” Structure in DEM of Difference

Figs. 5 to 8 represent DEMs of difference for the full test object where distinctive radial “domes” appear to be approximately located to the left of the centre of DEMs. They are caused by residual systematic effects arising from slightly inaccurate radial lens distortion parameters and have also been noted in past work (Stojic et al., 1998; Chandler et al., 2003, 2005). A theoretical proof explaining them was given in Fryer and Mitchell (1987). This confirms that any uncorrected residual x parallaxes will create a systematic offset in computed elevations, causing a flat object to appear curved.

The radial domes (maximum elevation of 2 mm) clearly affect the accuracy statistic estimated for the central test object. The achieved accuracy for the sensors is approximately 1.4 mm (average mean error) for the central area tested. By removing these systematic errors in difference images, the cameras will be certainly capable of achieving an improved accuracy, perhaps approaching the theoretical optimum of 0.5 mm at this camera-to-object distance of 1.5 m.

The variation in radial lens distortion for sensor 5 using various sets of IOP are shown in Fig. 9. The differences between these curves and the mean curve never exceed 7 μ m and even these extremes were achieved at the very edges of the image format. These results correspond

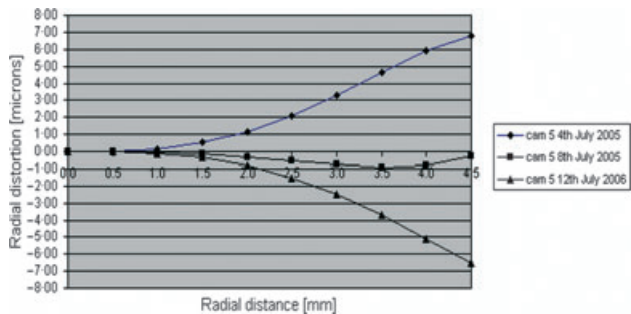


FIG. 9. Radial distortion curves showing differences with respect to a mean curve for camera 5 and three sets of IOP.

closely to the findings of Robson and Gyory (2006) in which the variations in distortion for eight sensors of a panoramic camera cluster have been investigated.

Reviewing the results summarised in Tables II to V and Fig. 9, the cameras achieved similar accuracy whichever combination of camera and IOP was used. This level of accuracy is suitable for routine measurement of textured surfaces and DEM generation to an accuracy of 2 mm. Tests have demonstrated remarkable temporal stability and manufacturing consistency of the cameras. Variations in calibration parameters for these sensors are generally not significant when they are used at the level of accuracy described. This finding agrees with the experimental camera calibration tests carried out by Remondino and Fraser (2006).

CONCLUSION

The work presented in this paper has explored and successfully identified the temporal stability and manufacturing consistency of the Nikon Coolpix 5400 digital camera over a 1-year period. This type of camera is capable of generating DEMs to an accuracy of 1.4 mm, from a distance of 1.5 m using IOP derived through self-calibration using imagery obtained by any of these cameras. This result is highly significant, as it implies that a “generic” distortion curve may well be applicable for all Nikon 5400 cameras (based on the sample of seven). In addition, such accuracies could be suitable for many applications. This paper also identified existing systematic errors in difference images which are caused by slightly inaccurate lens distortion parameters being estimated by the self-calibration approach. These effectively constrain the accuracies achievable. Further experimental work will be conducted to see if it is possible to reduce these effects, and will be reported in a future paper.

ACKNOWLEDGEMENTS

The authors would like to acknowledge the work of Dr Tertia Barnett, formerly Chair of the Northumberland and Durham Rock Art Project (Northumberland County Council) and also the Engineering and Physical Sciences Research Council (EPSRC) for the first author’s studentship.

REFERENCES

- AHMAD, A. and CHANDLER, J. H., 1999. Photogrammetric capabilities of the Kodak DC40, DCS420 and DCS460 digital cameras. *Photogrammetric Record*, 16(94): 601–615.
- BARNETT, T., 2006. *Northumberland and Durham Rock Art Project*. <http://pscm.northumberland.gov.uk/pls/portal92/docs/2091.pdf> [Accessed 10th August 2006].
- BEYER, H. A., UFFENKAMP, V. and VAN DER VLUGT, G., 1995. Quality control in industry with digital photogrammetry. *Optical 3-D Measurement Techniques III* (Eds. A. Gruen and H. Kahmen). Wichmann, Heidelberg. 533 pages: 29–38.
- BOSCH, R., KÜLÜR, S. and GÜLCH, E., 2005. Non-metric camera calibration and documentation of historical buildings. *CIPA XX International Symposium*, Torino. 990 pages: 142–147.
- BROWN, D. C. and DOLD, J., 1995. V-STARS—a system for digital industrial photogrammetry. *Optical 3-D Measurement Techniques III* (Eds. A. Gruen and H. Kahmen). Wichmann, Heidelberg. 533 pages: 12–21.
- CHANDLER, J. H. and CLARK, J. S., 1992. The archival photogrammetric technique: further application and development. *Photogrammetric Record*, 14(80): 241–247.
- CHANDLER, J. H., BUFFIN-BÉLANGER, T., RICE, S., REID, I. and GRAHAM, D. J., 2003. The accuracy of a river bed moulding/casting system and the effectiveness of a low-cost digital camera for recording river bed fabric. *Photogrammetric Record*, 18(103): 209–223.
- CHANDLER, J. H., FRYER, J. G. and JACK, A., 2005. Metric capabilities of low-cost digital cameras for close range surface measurement. *Photogrammetric Record*, 20(109): 12–26.
- CHANDLER, J. H., BRYAN, P. and FRYER, J. G., 2007. The development and application of a simple methodology for recording rock art using consumer-grade digital cameras. *Photogrammetric Record*, 22(117): 10–21.

- CLARKE, T. A. and FRYER, J. G., 1998. The development of camera calibration methods and models. *Photogrammetric Record*, 16(91): 51–66.
- DOLD, J. and PEIPE, J., 1996. High resolution data acquisition to observe moving objects. *International Archives of Photogrammetry and Remote Sensing*, 31(B5): 471–474.
- ERDAS, 2002. *IMAGINE OrthoBASE User's Guide*. Leica Geosystems, Atlanta. 483 pages: 341.
- FRASER, C. S., 1982. Film unflatness effects in analytical non-metric photogrammetry. *International Archives of Photogrammetry and Remote Sensing*, 24(5): 156–166.
- FRASER, C. S., SHORTIS, M. R. and GANCI, G., 1995. Multi-sensor system self-calibration. *Videometrics IV. SPIE* 2598:2–18.
- FRYER, J. G. and MITCHELL, H. L., 1987. Radial distortion and close range stereophotogrammetry. *Australian Journal of Geodesy, Photogrammetry and Surveying*, 46/47: 123–138.
- FRYER, J. G., MITCHELL, H. and CHANDLER, J. H., 2007. *Applications of 3D Measurement from Images*. Whittles, Caithness. 384 pages.
- GRANSHAW, S. I., 1980. Bundle adjustment methods in engineering photogrammetry. *Photogrammetric Record*, 10(56): 181–207.
- HABIB, A. and MORGAN, M., 2005. Stability analysis and geometric calibration of off-the-shelf digital cameras. *Photogrammetric Engineering & Remote Sensing*, 71(6): 733–741.
- HABIB, A., PULLIVELLI, A., MITSHITA, E., GHANMA, M. and KIM, E.-M., 2006. Stability analysis of low-cost digital cameras for aerial mapping using different georeferencing techniques. *Photogrammetric Record*, 21(113): 29–43.
- KENEFICK, J. F., GYER, M. S. and HARP, B. F., 1972. Analytical self-calibration. *Photogrammetric Engineering*, 38(11): 1117–1126.
- LI, Z., 1988. On the measure of digital terrain model accuracy. *Photogrammetric Record*, 12(72): 873–877.
- LICHTI, D. D. and CHAPMAN, M. A., 1997. Constrained FEM self calibration. *Photogrammetric Engineering & Remote Sensing*, 63(9): 1111–1119.
- MILLS, J. P., SCHNEIDER, D., BARBER, D. M. and BRYAN, P. G., 2003. Geometric assessment of the Kodak DCS Pro Back. *Photogrammetric Record*, 18(103): 193–208.
- MIYATSUKA, Y., 1996. Archaeological real-time photogrammetric system using digital still camera. *International Archives of Photogrammetry and Remote Sensing*, 31(B5): 374–377.
- PEIPE, J., 1995. Photogrammetric investigation of a 3000 × 2000 pixel high resolution still video camera. *International Archives of Photogrammetry and Remote Sensing*, 30(5W1): 36–39.
- REMONDINO, F. and FRASER, C., 2006. Digital camera calibration methods: considerations and comparisons. *International Archives of Photogrammetry, Remote Sensing and Spatial Information Sciences*, 36(5): 266–272.
- ROBSON, S. and GYORY, G., 2006. OpTag—a combined panoramic photogrammetric and radio frequency tagging system for monitoring passenger movements in airports. *International Archives of Photogrammetry, Remote Sensing and Spatial Information Sciences*. http://www.isprs.org/commission5/proceedings06/paper/1262_Dresden06.pdf [Accessed 29th November 2006].
- SCHNEIDER, C.-T., 1996. DPA-WIN—a PC based digital photogrammetric station for fast and flexible on-site measurement. *International Archives of Photogrammetry and Remote Sensing*, 31(B5): 530–533.
- SHORTIS, M. R., ROBSON, S. and BEYER, H. A., 1998. Principal point behaviour and calibration parameter models for Kodak DCS cameras. *Photogrammetric Record*, 16(92): 165–186.
- SHORTIS, M. R., OGLEBY, C. L., ROBSON, S., KARALIS, E. M. and BEYER, H. A., 2001. Calibration modeling and stability testing for the Kodak DC200 series digital still camera. *Videometrics and Optical Methods for 3D Shape Measurements. SPIE* 4309: 148–153.
- STOJIC, M., CHANDLER, J. H., ASHMORE, P. and LUCE, J., 1998. The assessment of sediment transport rates by automated digital photogrammetry. *Photogrammetric Engineering & Remote Sensing*, 64(5): 387–395.

Résumé

Il est bien connu que la précision des données que l'on peut tirer des caméras numériques du commerce se trouve limitée par l'incertitude de leur géométrie interne. On peut étalonner ces caméras mais il convient de vérifier soigneusement la validité de cet étalonnage dans le temps avant de les utiliser pour des déterminations photogrammétriques. On étudie dans cet article la stabilité géométrique et la reproductibilité de fabrication d'une caméra numérique typique et bon marché (Nikon Coolpix 5400) en estimant le degré de ressemblance des paramètres

d'orientation interne (POI) obtenus sur une période d'un an. En utilisant sept caméras identiques, on a pu calculer des Modèles Numériques d'Élévation (MNE) en utilisant des paramètres d'orientation interne différents et en comparer la précision. Pour obtenir les jeux de données correspondants, on s'est servi du logiciel « suite photogrammétrique » de Leica (LPS) et d'une compensation par faisceaux avec auto-étalonnage. Les résultats que l'on présente montrent l'aptitude de ces caméras à conserver leur géométrie interne en termes de stabilité dans le temps et de reproductibilité dans leur fabrication. Les « MNE des différences » mettent en évidence des erreurs systématiques résiduelles surfaciques en forme de dôme. Elles proviennent de petites inexactitudes dans l'estimation des paramètres de distorsion des objectifs et limitant effectivement la précision que l'on peut attendre avec cette classe de capteurs.

Zusammenfassung

Es ist allgemein bekannt, dass die unsichere innere Geometrie von digitalen Amateurkameras die Genauigkeit der aus den digitalen Bildern extrahierten Daten limitiert. Diese Kameras können zwar kalibriert werden, aber die Gültigkeitsdauer dieser Kalibrierungsparameter sollte vor der Verwendung für photogrammetrische Zwecke sorgfältig überprüft werden. Diese Veröffentlichung betrachtet die geometrische Stabilität und die Fertigungsstabilität einer typischen, kostengünstigen, digitalen Kamera (Nikon Coolpix 5400) durch Beurteilung des Ähnlichkeitsgrades der inneren Orientierungsparameter, welche über einen Zeitraum von einem Jahr ermittelt wurden. Die ermittelten inneren Orientierungen von sieben identischen Kameras wurden benutzt, um Digitale Höhenmodelle zu extrahieren und ihre Genauigkeiten zu vergleichen. Ein unabhängiges Programm zur Bündeltriangulation (GAP) sowie die Leica Photogrammetry Suite (LPS) Software wurden benutzt, um diese Höhenmodelle bereitzustellen. Ergebnisse werden präsentiert, welche das Potential dieser Kameras zeigen, ihre geometrische Stabilität und ihre Fertigungsstabilität beizubehalten. Diese Studie identifiziert aber auch Oberflächen mit systematischen Fehlern oder "Kuppeln", sichtbar in dem Differenzbetrag digitaler Höhenmodelle. Diese werden durch ungenau berechnete radiale Verzeichnungsparameter verursacht und limitieren die erreichbare Genauigkeit mit diesen Kameras.

Resumen

Es conocido el hecho de que lo incierto de la geometría interna de las cámaras digitales de consumo limita la exactitud de los datos que se pueden extraer de ellas. Dichas cámaras pueden calibrarse, pero la validez temporal de los datos de calibración ha de comprobarse concienzudamente antes de realizar medidas fotogramétricas. El artículo examina la estabilidad geométrica y la consistencia de fabricación de una cámara típica de bajo coste (Nikon Coolpix 5400) en base a estimar el grado de similitud entre los parámetros de orientación interna en el periodo de un año. Para ello se calculan Modelos de Elevaciones del Terreno con parámetros de orientación interna que difieren entre sí, y se comparan los resultados de precisión obtenidos para siete cámaras idénticas. Para la generación de las pruebas se utilizó un programa independiente de ajuste por haces con autocalibración y el sistema "Leica Photogrammetric Suite (LPS)". Se presentan resultados que muestran el potencial de esas cámaras para mantener su geometría interna en

términos de estabilidad temporal y consistencia de fabricación. El estudio identifica también superficies de errores sistemáticos residuales o “domos” que son discernibles calculando las diferencias entre modelos de elevación. Dichos errores son debidos a estimaciones poco precisas de los parámetros de distorsión de las lentes y delimitan las precisiones alcanzables con esa clase de sensores.